Enhancing the Nonlinear Optical Response Using Multifrequency Gold-Nanowire Antennas

Hayk Harutyunyan, Giorgio Volpe, Romain Quidant, and Lukas Novotny

Phys. Rev. Lett. **108**, 217403 — Published 23 May 2012

DOI: 10.1103/PhysRevLett.108.217403

Enhancing the nonlinear optical response using multifrequency gold nanowire antennas

Hayk Harutyunyan[1], Giorgio Volpe[2], Romain Quidant[2,3], and Lukas Novotny[1*]
[1] *Institute of Optics, University of Rochester, Rochester, NY 14627, USA*
[2] *ICFO-Institut de Ciencies Fotoniques, Mediterranean Technology Park, 08860 Castelldefels (Barcelona), Spain and*
[3] *ICREA-Institució Catalana de Recerca i Estudis Avançats, 08010 Barcelona, Spain*

We introduce and experimentally demonstrate the concept of multifrequency optical antennas that are designed for controlling the nonlinear response of plasmonic structures. These antennas consist of two arms of different lengths, each resonant with one of the incoming frequencies. They are embedded in a nonlinear medium (indium tin oxide) that acts as a receiver. Because the two arms have different spectral resonances, tuning of the antenna gap size has minimal effect on the *linear* optical properties. However, it strongly affects the *nonlinear* response. Thus, by employing antenna elements with different spectral resonances we provide a strategy to decouple the nonlinear response of nanomaterials from their linear optical properties.

PACS numbers: 78.47.N-, 78.67.Bf,73.20.Mf,73.21.-b,42.65.Hw

Optical antennas provide a means to transduce localized fields into free propagating optical radiation, and vice versa [1]. So far, most of the implemented antenna structures operate in the linear regime, that is, the polarization currents depend linearly on the excitation field. The illumination of an optical antenna by an incident radiation generates strongly enhanced localized fields governed by distinct plasmon resonances [2–4]. These local fields can be further enhanced and controlled by antennas made of multiple elements. For example, gap antennas, consisting of two arms of equal length separated by a tiny gap, have been used to control both the linear response and the nonlinear response [5–7]. Recently, *nonlinear* optical antennas have been discussed theoretically for modulation and switching purposes [8–10], however, the nonlinear response can be complex and it is not *a priori* clear what the best design strategies are to optimize the nonlinear response [11]. A figure of merit for nonlinear materials is the strength of the nonlinear response relative to the linear response of the material [12, 13]. Typically, the nonlinear response depends on a strong linear response [7]. Here we show that this is not generally the case and that we are able to enhance the nonlinear response without increasing the linear response.

The multifrequency antenna consists of two metal arms of different lengths and separated by a gap that is filled by a nonlinear optical material (Fig. 1). The fields $E_S(\omega_1)$ and $E_S(\omega_2)$ received by the two antenna arms overlap in the gap region where they simultaneously interact with the nonlinear medium. The lengths of the metal arms are chosen such that a half-wave resonance is established at frequencies ω_1 and ω_2, respectively [14–17]. The nonlinear medium can be viewed as a localized receiver which converts the input signals at frequencies ω_1 and ω_2 into an output signal centered at frequency ω_3 through a third-order nonlinear frequency mixing process referred to as four-wave mixing (4WM) [18]. While there is no gap enhancement effect in the linear regime for either of the incoming wavelengths, the nonlinear response is strongly dependent on the gap size proving the purely nonlinear nature of these resonant antennas.

In our experiments the antenna structures were fabricated on ITO-coated glass substrates using standard positive-resist e-beam lithography. The samples consisted of antenna arrays with varying antenna arm length and gap size. As shown in Fig. 1 two ∼200 fs infrared pulse trains $E_0(\omega_1)$ and $E_0(\omega_2)$, at 800 and 1150 nm respectively, were focused on a single antenna structure resulting in spot sizes comparable in size to the

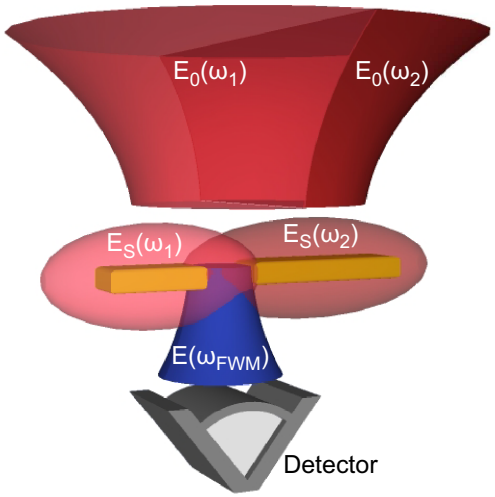

FIG. 1: Illustration of the resonant nonlinear frequency conversion experiment. Two excitation fields $E_0(\omega_1)$, $E_0(\omega_2)$ with different near-infrared frequencies are received by a linear gap antenna with different arm lengths. Each arm is resonant with one of the incoming frequencies. The antenna converts the input signals into an output signal centered at a new frequency $\omega_{4\mathrm{wm}}$, which is subsequently recorded by a detector.

dimensions of the antennas used in the experiments (210 nm to 510 nm). The distance between adjacent antennas was set to 4 μm to avoid any significant coupling effects. In a typical experiment, the sample was raster scanned through the laser focus and the signal was collected through the same focusing objective. For nonlinear measurements, the laser pulses were overlapped in space and time and the spectrum of scattered radiation was recorded with a CCD-coupled spectrometer (Fig. 1). For every image pixel a full spectrum was acquired. The spectra were then fitted with a narrow Lorentzian line shape function and a broad polynomial, from which we extracted the magnitudes of 4WM and two-photon excited luminescence (TPL). For determining the linear resonances of the antenna arms, dark-field linear scattering measurements were performed by using spatial filtering in the Fourier plane of the objective lens to reject laser light reflected from the glass-air interface. The light scattered by the antennas was detected by an APD. Because the backaperture of the objective was underfilled for the dark-field measurements the resulting focal laser spot sizes were on the order of a few microns, significantly larger than the diffraction limit. The polarization of both beams was aligned in direction of the antenna arms and the average power was on the order of $50-300\,\mu$W (peak intensities of $0.2-1.2\,\mathrm{GW/cm^2}$).

Let us first theoretically analyze the behavior of the nonlinear optical antenna. Fig. 2 shows the electromagnetic field distribution near an optical antenna made of two gold arms of lengths 80 nm and 140 nm respectively. The width of the antenna arms is 40 nm and their separation is 20 nm. The two antenna arms are embedded in a nonlinear medium with dielectric constant $\varepsilon = 2.89$ (ITO) and third-order susceptibility $\chi^{(3)} = 2.16\times10^{-18}\,m^2/V^2$, giving rise to an instantaneous nonlinear response [19]. As shown in Fig. 2(a), the field at wavelength $\lambda_1 = 780$ nm is resonant with the short antenna arm and gives rise to an enhanced field that is localized near the short antenna arm. On the other hand, the field at wavelength $\lambda_2 = 1100$ nm is resonant with and localized near the long antenna arm (c.f. Fig. 2b). The two enhanced fields overlap in the gap region where they induce a nonlinear polarization

$$\mathbf{P}^{(3)}(\omega_3) = \varepsilon_o\,\chi^{(3)}(-\omega_3;\omega_1,\omega_1,-\omega_2)\;\mathbf{E}_1\;\mathbf{E}_1\;\mathbf{E}_2^*\,, \quad (1)$$

which in turn gives rise to radiation at the frequency $\omega_3 = 2\omega_1 - \omega_2$. Fig. 2(c) depicts $|\mathbf{P}^{(3)}|^2$ near the optical antenna for an isotropic nonlinear material. The linecut in the figure shows that nonlinear signal generation is mostly localized to the gap region. We neglect the nonlinear response of the two gold arms because the exciting fields penetrate only weakly into the material (c.f. Fig. 2a,b) and therefore predominantly interact with the nonlinear medium surrounding the antenna arms. Thus, due to the asymmetry of the antenna design

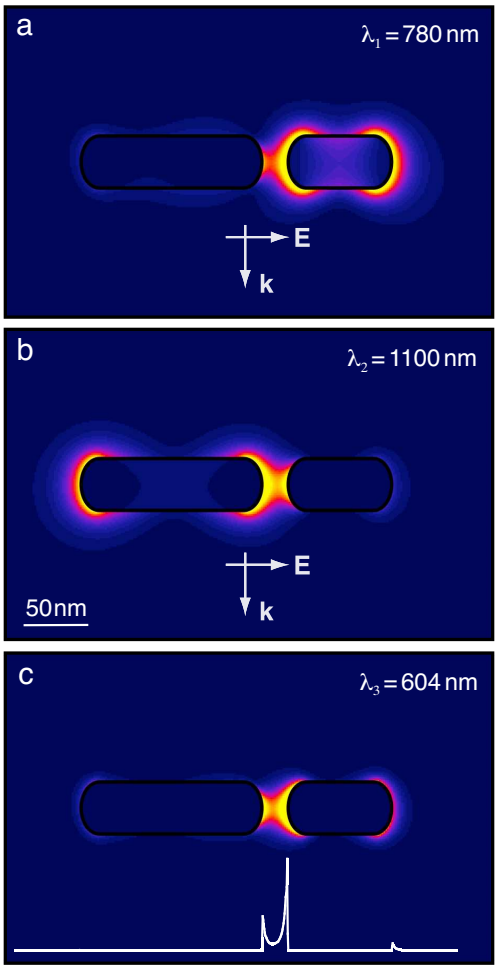

FIG. 2: Field distribution near an optical antenna made of two gold arms of length 80 nm and 140 nm, respectively, embedded in a nonlinear medium with dielectric constant $\varepsilon = 2.89$ (ITO). (a,b) Square modulus of electric field (E^2). The antenna is irradiated by plane waves of frequencies $\omega_1 = 2\pi c/\lambda_1$ and $\omega_2 = 2\pi c/\lambda_2$, respectively. (c) Square modulus of nonlinear polarization $|\mathbf{P}^{(3)}|^2$ at the frequency $\omega_3 = 2\omega_1 - \omega_2$. The white curve is a linecut along the axis of the antenna, showing that the nonlinear signal is almost entirely generated in the gap of the antenna.

the near-fields contributing to the linear (Fig. 2a, b) and nonlinear (Fig. 2c) optical response have different spatial distribution. This allows independent tuning of the two processes.

The spectral dependence of the nonlinear optical antenna is rendered in Fig. 3. The three curves show the square modulus of the electric field (E^2) normalized by the incident field intensity (E_o^2) for the short antenna arm alone (dashed line), the long antenna arm alone (dotted curve), and for both antenna arms (solid curve). For the two isolated antenna arms the field is evaluated at a distance of 1 nm from the endpoints of the antenna arms, and for the antenna consisting of both arms the

field is evaluated in the gap at the midpoint between the arms. The curves reveal that the short and long antenna arms exhibit half-wave resonances at $\lambda_1 = 780\,\text{nm}$ and $\lambda_2 = 1100\,\text{nm}$, respectively. The interaction between the two antenna arms slightly shifts the two resonances and increases the frequency splitting [14]. However, it is evident that the interaction is weak and that the spectral dependence of the two antenna arms is not significantly affected. To experimentally verify this observation we have performed linear scattering measurements on antennas. First, the lengths of antenna arms resonant with our excitation wavelengths at $\lambda_1 = 800\,\text{nm}$ and $\lambda_1 = 1150\,\text{nm}$ were identified by dark-field imaging of antennas of different arm lengths (data not shown). Then, the linear response of structures with fixed arm lengths, but varying gap size, was measured. Figure 3 (b) and (c) show the dark-field linear scattering of the same resonant antennas when only the size of the gap is varied from 20nm to 80 nm in 10 nm steps. In both images the scattering amplitude is nearly constant proving that the linear interaction is virtually absent in far-field measurements. Higher order plasmonic modes are not expected to play a major role under current experimental conditions due to the relatively small size of the antenna elements [5]. This was verified by

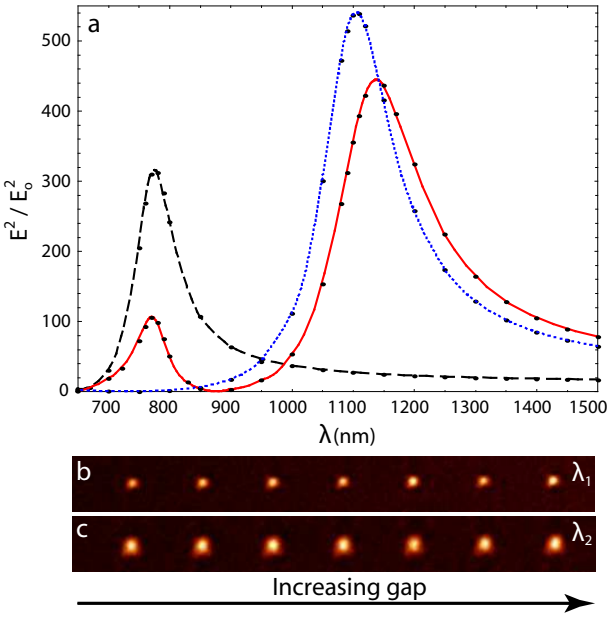

FIG. 3: Spectral dependence of the nonlinear optical antenna. (a) Dashed curve: short antenna arm alone; dotted curve: long antenna arm alone; solid curve: both antenna arms. The dashed and dotted curves correspond to the square modulus of the field (E^2) evaluated at a distance of 1 nm from the endpoints of the antenna arms. The solid curve corresponds to the E^2 evaluated at the midpoint between the two antenna arms. (b) and (c) dark-field scattering images of antennas with fixed arm lengths of 110 nm and 210 nm, at the two excitation wavelengths $\lambda_1 = 800\,\text{nm}$ and $\lambda_2 = 1150\,\text{nm}$.

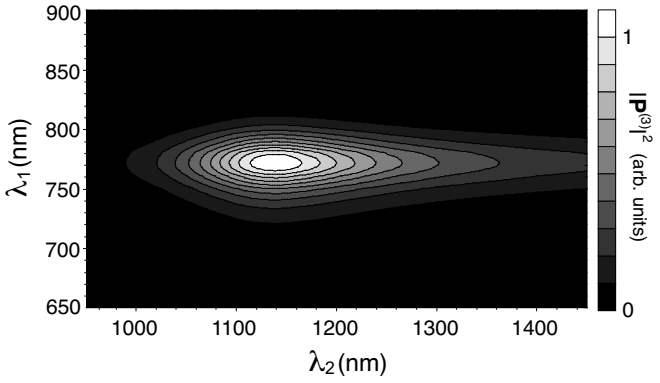

FIG. 4: Efficiency of frequency conversion of the antenna shown in 3 as a function of input wavelengths. The figure shows contours of $|\mathbf{P}^{(3)}(\lambda_1, \lambda_2)|^2$, which is proportional to the frequency conversion efficiency.

linear scattering measurements at 633 nm, close to 4WM emission wavelength (615nm), where no measurable gap dependence of the scattered signal was observed.

We next evaluate the efficiency of frequency conversion as a function of the two incident wavelengths λ_1 and λ_2. For simplicity we assume that the $\chi^{(3)}$ is frequency independent. The frequency conversion efficiency is proportional to the square modulus of the nonlinear polarization and is shown in Fig. 4. The nonlinear spectral response from composite materials can be complex due to the strong coupling between the plasmonic modes [11]. However, from Fig. 4 it is evident that in the case of spectrally detuned antenna elements the overall nonlinear response is still governed by the plasmonic resonances of the individual elements and the frequency conversion efficiency is the highest if the two incident wavelengths are resonant with the two antenna arms.

To test if the nonlinear response of the antennas indeed shows different behavior as compared to their linear response as predicted by the theoretical calculations shown in Fig. 2 we carried out experiments of frequency conversion with different antenna geometries (Fig. 5). Here each arm length was chosen according to the linear measurements to be in resonance with one of the excitation wavelengths and the gap size was again varied from 20 nm to 80 nm. In difference to our linear scattering experiments, the 4WM signal strongly depends on the size of the gap. The signal is strongest for the smallest gap size and vanishes for large gaps (Fig. 5). On the other hand, if the antenna arms are *not* resonant with the excitation wavelengths we find that the 4WM signal reduces significantly and no longer depends on the gap size (data not shown). Thus, by employing antenna elements with different spectral resonances we provide a

strategy to tune the nonlinear response independent of the linear properties. This behavior is expected to break down in the quasi-static regime where the resonances are no longer size-dependent [20]. The results shown in Fig. 5 have been verified for different antenna arrays. While there are slight variations among the data points due to fabrication uncertainties (see inset of Fig. 5) the above mentioned trends were consistently observed for all measured antenna arrays [21].

In our experiments the antennas were resting on a nonlinear substrate rather than being embedded in it as in the calculations presented above. This difference however, has proven to have little or no influence on the nonlinear response of very similar nanoentenna-ITO hybrid systems [22]. Thus, while embedding our samples in ITO or any other highly nonlinear medium might have increased the efficiency of frequency conversion, we do not expect any qualitative changes in the behavior of the nonlinear signal. The gap dependence of the 4WM signal in resonant antennas is a direct evidence that the signal is generated in the nonlinear material in the gap region, i.e. the nonlinear substrate and the end facets of the antenna arms. It is also interesting to note that we did not measure any reproducible gap dependence of the emitted two-photon excited luminescence (TPL) signal. TPL is a nonlinear process that does not require multifrequency excitation and therefore is expected to be significantly less sensitive to the relative positions of the antenna elements. Similarly, if the two antenna arms are excited non-resonantly, most of the residual 4WM signal originates from the individual antenna arms and hence does not depend on the gap size.

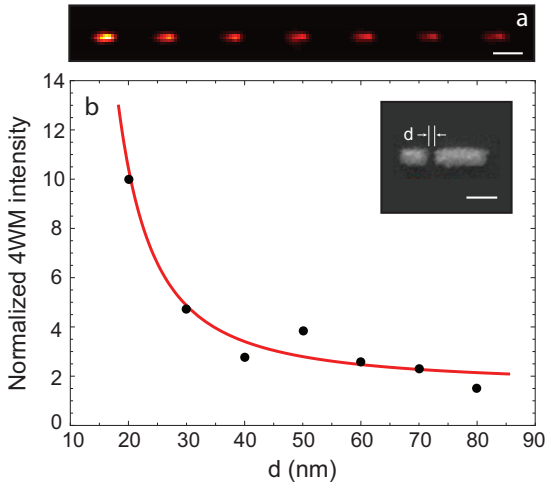

FIG. 5: Dependence of 4WM on antenna gap. (a) 4WM images of a sequence of antennas with fixed arm lengths (110 nm and 210 nm) and varying gap size d. The gap is varied from 20 nm (left) to 80 nm (right). Scalebar 1 μm. (b) Total 4WM signal normalized to the linear response shown in Figs. 3(b) and (c) [21]. The solid line is an exponential fitting function. The inset shows an SEM image of an asymmetric gold antenna. Scalebar 100 nm.

In conclusion we have introduced the concept of resonant nonlinear antennas and have experimentally demonstrated its realization at optical frequencies. The use of nonlinear materials in combination with traditional noble metal nanostructures provides a framework for nonlinear optical signal generation. The approach developed here holds promise for applications such as on-chip optical frequency conversion and design of metamaterials with enhanced nonlinear response.

This research was funded by the U.S. Department of Energy (grant DE-FG02-01ER15204), the National Science Foundation (grant ECCS-0918416), ERC-2010-StG Plasmolight (grant:259196) and Fundació privada CELLEX. We thank Pieter Kik, Palash Bharadwaj and Zack Lapin for valuable input and fruitful discussions.

* URL: `www.nano-optics.org`

[1] L. Novotny and N. F. van Hulst, Nature Phot. **5**, 83 (2011).
[2] J. A. Schuller, E. Barnard, W. Cai, Y. C. Jun, J. White, and M. L. Brongersma, Nature Mat. **9**, 193 (2010).
[3] H. A. Atwater and A. Polman, Nature Mat. **9**, 205 (2010).
[4] M. W. Knight, H. Sobhani, P. Nordlander, N. J. Halas, Science **332**, 702 (2011).
[5] P. Ghenuche *et al.*, Phys. Rev. Lett. **101**, 116805 (2008).
[6] P. Mühlschlegel, H.-J. Eisler, O. J. F. Martin, B. Hecht, and D. W. Pohl, Science **308**, 1607 (2005).
[7] M. Danckwerts and L. Novotny, Phys. Rev. Lett. **98**, 026104 (2007).
[8] F. Zhou, Z. L. Y. Liu, and Y. Xia, Opt. Express **18**, 13337 (2010).
[9] P.-Y. Chen and A. Alù, Phys. Rev. B **82**, 235405 (2010).
[10] N. Large, M. Abb, J. Aizpurua, and O. L. Muskens, Nano Lett. **10**, 1741 (2010).
[11] T. Utikal *et al.*, Phys. Rev. Lett. **106**, 133901 (2011).
[12] D. C. Kohlgraf-Owens and P. G. Kik, Opt. Expr. **16**, 16823 (2008).
[13] D. C. Kohlgraf-Owens and P. G. Kik, Opt. Expr. **17**, 15032 (2009).
[14] J. Aizpurua, G. W. Bryant, L. J. Richter, F. J. G. de Abajo, B. K. Kelley, and T. Mallouk, Phys. Rev. B **71**, 235420 (2005).
[15] L. Novotny, Phys. Rev. Lett. **98**, 266802 (2007).
[16] J.-S. Huang, J. Kern, P. Geisler, P. Weinmann, M. Kamp, A. Forchel, P. Biagioni and B. Hecht, Nano Lett. **10**, 2105 (2010).
[17] R. L. Olmon *et al.*, Opt. Expr. **16**, 20295 (2008).
[18] Y. R. Shen, *The Principles of Nonlinear Optics* (Wiley, New York, USA, 1984).
[19] J. L. Humphrey and D. Kuciauskas, J. Appl. Phys. **100**, 113123 (2006).
[20] K. Li, M. I. Stockman, and D. J. Bergman, Phys. Rev. Lett. **91**, 227402 (2003).
[21] See Supplemental Material at [URL will be inserted by publisher] for normalization procedure of the nonlinear

response and statistics of experimental data.
[22] M. Abb, P. Albella, J. Aizpurua, and O. L. Muskens, Nano Lett. **11**, 2457 (2011).